On Channel-Aware Frequency-Domain Scheduling With QoS Support for Uplink Transmission in LTE Systems

Lung-Han Hsu and Hsi-Lu Chao
Department of Computer Science
National Chiao Tung University, Hsinchu, Taiwan

Abstract—**Due to the power consumption issue of user equipment (UE), Single-Carrier FDMA (SC-FDMA) has been selected as the uplink multiple access scheme of 3GPP Long Term Evolution (LTE). Similar to OFDMA downlink, SC-FDMA enables multiple UEs to be served simultaneously in uplink as well. However, the single carrier characteristic requires that all the allocated subcarriers to a UE must be contiguous in frequency with each time slot. Moreover, a UE should adopt the same modulation and coding scheme at all allocated subcarriers. These two constraints do limit the scheduling flexibility. In this paper, we formulate the UL scheduling problem with proportional fairness support by taking two constraints into consideration. Since this optimization had been proven to be an NP-hard problem, we further develop one heuristic algorithm. We demonstrate that competitive performance can be achieved in terms of system throughput, which is evaluated by using 3GPP LTE system model simulations.**

Keywords — **LTE, uplink, SC-FDMA, resource allocation, contiguous constraint, robust rate constraint, channel-aware scheduling, proportional fairness**

I. INTRODUCTION

Due to the characteristics of robustness to multipath fading, and higher spectral efficiency and bandwidth scalability, Orthogonal Frequency Division Multiple Access (OFDMA) has been adopted as the 3GPP Long Term Evolution (LTE) downlink (DL) radio access technology. However, an undesirable high peak-to-average power ratio (PAPR) is a serious concern to uplink (UL), since power consumption is still a key consideration to mobile devices. As a result, Single-Carrier FDMA (SC-FDMA), which keeps most of the advantages of OFDMA while having significantly lower PAPR, has been selected as the LTE UL multiple access technology.

In the LTE cellular system, the available spectrum is divided into resource blocks (RBs). Each RB consists of 12 adjacent subcarriers, and its time duration, known as Transmission Time Interval (TTI), is 1 ms [1]. In an OFDMA-based multi-user system, RBs are allocated to the UEs that experience good channel conditions for maximizing the multi-user diversity gain and increase the cell throughput. Therefore, channel dependent scheduling (CDS) works well for the LTE DL subsystem. Contrarily, CDS may be not suitable for the LTE UL subsystem due to two inherent constraints: contiguity constraint and robust rate constraint.

The contiguity constraint means that, for LTE UL, RBs are allocated to a single UE in a contiguous manner due to the requirement of SC-FDMA [2]. This significantly reduces the degree of freedom in resource allocation. On the other hand, the robust rate constraint is that a UE must adopt the same modulation and coding scheme (MCS) for all allocated RBs [3]. Therefore, a UE can only utilize the most robust RB rate at its allocated RBs. Both constraints affect the performance of UL resource allocation in terms of throughput. Most literature only takes contiguity constraint into consideration to design frequency-domain scheduling algorithms for LTE UL [4-7], while ignoring the impact of robust rate constraint. In the following, we first describe the related work studying the scheduling problem of LTE UL transmission, and then the problem description and our motivation.

A. Literature Study

Scheduling algorithms for LTE UL with QoS support in literature mainly focus on proportional fairness (PF). The reason is that PF aims at balancing the system throughput performance and user fairness [4]. In [5], the authors proposed four practical heuristic algorithms with proportional fairness support. First Maximum Expansion (FME), which also supports proportional fairness, was proposed in [6] and the scheduler maintains a channel dependent matrix to do scheduling. In [6], the scheduler first searches for the largest matrix element value, say element (i, j), and then assigns RB_j to UE_i. Followed, the scheduler performs RB expansion in either direction, which is determined by the element value.

In [7], considering contiguity constraint and robust rate constraint, the authors proposed two heuristic scheduling algorithms, named TTRA and STRA. TTRA consists of two tiers: the first tier allocation is exactly a regular CDS scheduling; the second tier allocation fine-tunes the tier-one scheduling result for improving the sum throughput performance afterwards. Though TTRA contributes better performance than regular CDS algorithms, it may cost much time to run two-tier scheduling operations. The main characteristic of STRA is that it performs contiguous RB assignment and sum throughput improvement simultaneously.

[5-6] have taken PF in to consideration, but UEs are allowed to operate at different MCS modes at their allocated RBs. In other words, a UE can change its RB rate per-RB basis. This is an impractical assumption because the modulation function in the physical layer can select only one MCS mode, this MCS mode will apply to allocated RBs. However, [7] have considered robust rate constraint, but it doesn't consider user fairness. It may let some UEs to starve, because their channel condition is too bad to allocate RB to them.

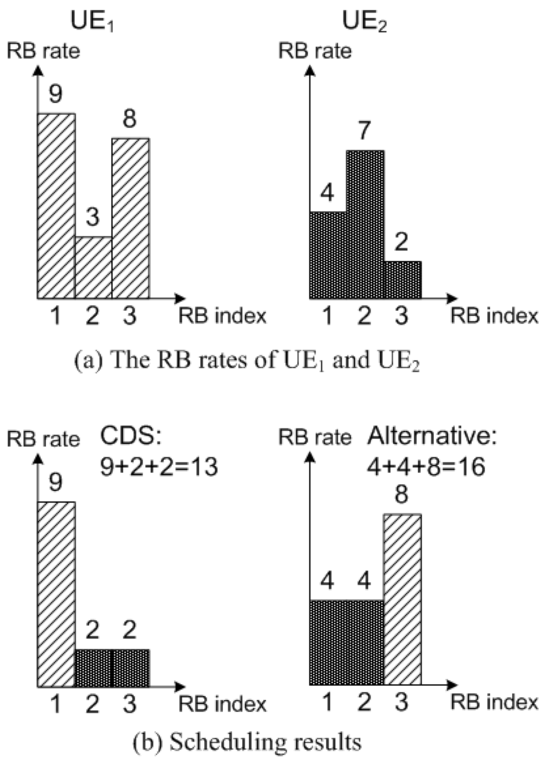

Fig. 1. The effect of the first RB to be allocated on the performance of sum RB rate

B. Problem Description and Motivation

The scheduling criterion adopted in most approaches is the measured SNR value (in the rest of this paper, the measured SNR value is interpreted as RB rate). However, this concept may not always be suitable for UL scheduling. We use an example to illustrate the reason. An example is shown in Fig. 1. In this example, there are three RBs and two UEs. The RB rates of UE_1 and UE_2 are (9, 3, 8) and (4, 7, 2), respectively, shown in Fig. 1(a). Let $r_{i,j}$ indicate the RB rate of UE_i at RB_j. Since the largest RB rate is $r_{1,1}$, the CDS-based scheduler allocates RB_1 to UE_1. Followed, considering the contiguity constraint and comparing the RB rates of UE_1 and UE_2 at RB_2, the scheduler allocates RB_2 to UE_2 due to ($r_{1,2}$ =3) < ($r_{2,2}$ =7). Again, because of the contiguity constraint, RB_3 can only be allocated to UE_2, even though ($r_{1,3}$ =8) > ($r_{2,3}$ =2). As a result, the sum RB rate of conventional rate-based scheduling algorithms is 9+2+2=13, as shown in Fig. 1(b). Contrarily, an alternative scheduler chooses the RB which has the maximum difference between the largest and the second largest RB rates to perform scheduling. In this example, $|r_{1,1}$-$r_{2,1}|$=5, $|r_{1,2}$-$r_{2,2}|$=4, and $|r_{1,3}$-$r_{2,3}|$=6, therefore, the scheduler performs scheduling operations on RB_3. Since UE_1 has a larger RB rate than UE_2, RB_3 is allocated to UE_1. Assume both RB_1 and RB_2 are allocated to UE_2, the sum RB rate would be 4+4+8=16. This observation inspires us to re-define a suitable scheduling criterion for LTE UL transmissions, and design a scheduling algorithm as well to support proportional fairness.

The paper is organized as follows. The system model of the LTE UL subsystem and the problem formulation are presented in Section II. The designed heuristic scheduling algorithm is described in Section III. The simulation results are presented and discussed in Section IV. Finally, the conclusion and future work are described in Section V.

II. System Model and Problem Formulation

In this section, we first describe the adopted LTE UL system. Followed, we formulate the scheduling problem.

A. System Model

We consider a cellular network which consists of a fixed serving eNodeB and *n* active UEs (denoted UE_1, UE_2, .., UE_n). The UL bandwidth per TTI of this cellular network is divided into *m* RBs (denoted RB_1, RB_2, .., RB_m). At each TTI, multiple contiguous RBs can be assigned to a single UE, while each RB can be assigned to at most one UE. A UE operates at the same MCS mode in all assigned RBs. Since channel conditions typically depend on channel frequencies, user locations, and time slots, each RB has user-dependent and time-varying channel conditions. The duty of RB allocation is performed by a frequency-domain scheduler, which is located in the eNodeB. Moreover, the scheduler performs resource allocation once per TTI. In order to improve fairness, we adopt proportional fairness (PF). The scheduling value in PF is current RB rates of UE divided by average RB rates. This method can improve fairness because that average RB rates is smaller means the UE got fewer radio resource previous time, and scheduling value of this UE this time can be larger. More radio resource can be allocated to those who have smaller average RB rate.

Let $\delta_{i,j}(t)$ and $F()$ be the measured SNR value of UE *i* on RB *j* at TTI *t* and the RB rate mapping function, respectively. Since RB is the smallest resource unit, herein we name the data bits carried in a RB "*RB rate*". We further let $r_{i,j}(t)$ indicate the number of bits carried in RB_j by UE_i at TTI *t*, and it indeed is the RB rate.

B. Problem Formulation

In our problem formulation, we consider Proportional Fairness (PF) to maximize the system throughput as well as to improve the fairness. Let $S_i(t)$ and $|S_i(t)|$ be the set and the number of assigned RBs of UE *i* at TTI *t*. $\bar{R}_i(t)$ and $r_i(t)$ are the average RB data of UE *i* from TTI 1 to TTI *t*. and its most robust RB rate among all allocated RBs at TTI *t*, respectively. We further let $x_{i,j}(t)$ be the allocation indicator: $x_{i,j}(t) = 1$ means that RB *j* is allocated to UE *i* at TTI *t*; 0 otherwise. Further, we define || be the AND operation.

Our objective is to maximize the sum PF-based throughput upon several constraints, i.e.,

$$\max \sum_i \sum_j \frac{x_{i,j}(t) r_i(t)}{\bar{R}_i(t-1)} \quad (1)$$

s.t.

$$\sum_{i=1}^{n} x_{i,j}(t) \leq 1, \forall j \quad (2)$$

$$|S_i(t)| = \sum_{j=1}^{m} x_{i,j}(t), \forall i \quad (3)$$

$$\sum_{i=1}^{n} |S_i(t)| \leq m, \forall S_i(t) \neq \emptyset \quad (4)$$

$$r_i(S_i(t)) = F(\min_{j \in S_i(t)} \delta_{i,j}) \quad (5)$$

$$\text{If}(x_{i,k}(t) = 1 \;||\; x_{i,k+1}(t) = 0), \quad (6)$$
$$\text{then} \quad x_{i,j}(t) = 0, k+2 \leq j \leq m$$

$$\text{If}(x_{i,k}(t) = 1 \mid\mid x_{i,k-1}(t) = 0), \quad \text{then} \quad x_{i,j}(t) = 0, 1 \leq j \leq k-2 \tag{7}$$

Eq. (2) indicates each RB_j can be assigned to at most one UE. Eq. (3) calculates the number of assigned RBs of UE_i at TTI t. Eq. (4) is to ensure the total allocated RBs should not exceed the supported UL bandwidth. Eq. (5) is the robust rate constraint, which can be turned into the robust RB rate and determined by the worst SNR value within the allocated RBs of UE_i. $\mathcal{F}$ function is to derive the corresponding RB rate from an SNR value. Eq. (6) and Eq. (7) mean that the allocated RBs to UE_i must be in contiguous manner. The numerical result of the proposed formulation will be presented and discussed in Sec. IV.

III. The Proposed Heuristic Algorithm

Before elaborating the operations of our approach in detail, we first introduce the defined parameters and maintained tables.

A. Parameters and Table

Several parameters and one table are defined and maintained for resource allocation.

(1) Original RB rate ($r_{i,j}(t)$): the maximum data bits that UE i can carry at RB j at TTI t.

(2) Constrained RB rate ($\hat{r}_{i,j}(t)$): the maximum data bits that UE i can carry at RB j at TTI t upon considering the contiguity and robust rate constraints.

(3) Average RB rate ($\bar{R}_i(t)$): the average data bits that UE i has transmitted until the t^{th} TTI.

(4) Window (w): the number of contiguous RBs which are considered together to determine the constrained RB rate of the centered RB. Herein we set w be an odd number, and each UE may have a different window size.

(5) Window-constrained RB rate ($\tilde{r}_{i,j}(t)$): the maximum data bits that UE i can carry in RB j at TTI t when applying window condition.

(6) Rate gap (Δ_i(t)): the difference of the largest and the second-largest RB rates of a specific RB i at TTI t.

Besides, the scheduler maintains a Rate Table (R-Table) for RB allocation. Each entry is for a (UE-RB) pair and has three fields: original RB rate, constrained RB rate, and window-constrained RB rate. How to construct the R-Table will be introduced in part B.

B. Resource Block Allocation

The designed algorithm consists of four phases: (1) R-Table initialization, (2) the first RB assignment and R-Table updates, (3) selection of next RB and UE candidates, and (4) sum rate estimation, as described below. To support proportional fairness (PF), when being granted RBs, the original RB rates of UE i on RB j at TTI t is $r_{i,j}(t) = \frac{r_{i,j}(t)}{\bar{R}_i(t-1)}$.

(1) Phase 1: R-Table initialization

The scheduler initializes $r_{i,j}(t)$, $\hat{r}_{i,j}(t)$, and $\tilde{r}_{i,j}(t)$ according to the SNR values reported by UEs and the mapping function between SNR values and MCS modes. Thus the steps of R-Table initialization are:

Step 1: $r_{i,j}(t)$= $\mathcal{F}(\delta_{i,j}(t))$, $\forall(i,j)$, i=1, 2,.., n; j=1, 2,…, m.

Step 2: Initially $\hat{r}_{i,j}(t) = r_{i,j}(t)$.

Step 3: $\tilde{r}_{i,j}(t)$=min $\{\hat{r}_{i,j-\frac{w-1}{2}}(t), \ldots, \hat{r}_{i,j}(t), \ldots, \hat{r}_{i,j+\frac{w-1}{2}}(t)\}$.

An example is shown in Fig. 2(a). In this example, we assume w=3; there are 3 UEs and 5 RBs. Furthermore, the RB rates are known, and $r_{1,j}(t)$=[3, 7, 10, 8, 4], $r_{2,j}(t)$=[3, 5, 2, 10, 5], and $r_{3,j}(t)$=[3, 2, 1, 3, 3], j=1, 2, .., 5. Initially, $\hat{r}_{1,j}(t)$=[3, 7, 10, 8, 4], $\hat{r}_{2,j}(t)$=[3, 5, 2, 10, 5], and $\hat{r}_{3,j}(t)$=[3, 2, 1, 3, 3]. Moreover, we use UE_1 as an example to illustrate how to derive the window-constrained RB rates. For RB_1, $\tilde{r}_{1,1}(t)$= min$\{\hat{r}_{1,1}(t), \hat{r}_{1,2}(t)\}$ = min {3, 7} = 3; for RB_2, $\tilde{r}_{1,2}(t)$ = min$\{\hat{r}_{1,1}(t), \hat{r}_{1,2}(t), \hat{r}_{1,3}(t)\}$ = min {3, 7, 10} = 3. Similarly, the window-constrained RB rates of RB_3, RB_4, and RB_5 are $\tilde{r}_{1,3}(t)$ = min$\{\hat{r}_{1,2}(t), \hat{r}_{1,3}(t), \hat{r}_{1,4}(t)\}$ = min {7, 10, 8} = 7, $\tilde{r}_{1,4}$ = min$\{\hat{r}_{1,3}(t), \hat{r}_{1,4}(t), \hat{r}_{1,5}(t)\}$ = min {10, 8, 4} = 4, $\tilde{r}_{1,5}(t)$ = min$\{\hat{r}_{1,4}(t), \hat{r}_{1,5}(t)\}$ = min {8, 4} = 4, accordingly.

(2) Phase 2: The first RB assignment and R-Table updates

The scheduler selects the RB which has the largest rate gap to be the first for allocation. Specifically, let $\tilde{r}_{i,j}(t)$ and $\tilde{r}_{k,j}(t)$ be the largest and second-largest window-constrained RB-rates of RB_j, $i \neq k$, respectively. The scheduler performs the following two operations to allocate the first RB:

Step 1: $\Delta_j(t) = \tilde{r}_{i,j}(t) - \tilde{r}_{k,j}(t)$, $\forall j$.

Step 2: $\arg_j \max\{\Delta_j(t)\}$, and RB_j is the first for resource allocation.

Step 3: Since UE_i has the largest window-constrained RB rate, RB_j is allocated to UE_i.

Step 4: $\mathcal{M} = \mathcal{M} - \{RB_j\}$, $\mathcal{M}' = \mathcal{M}' + \{RB_j\}$, $\mathcal{N} = \mathcal{N} - \{UE_i\}$, and $\mathcal{N}' = \mathcal{N}' + \{UE_i\}$.

Step 5: Update $\hat{r}_{i,l}(t)$ and all $\tilde{r}_{q,l}$, $q \neq i$ and $l \neq j$. Specifically, for the UE_i, adjust those $\hat{r}_{i,l}(t) > \hat{r}_{i,j}(t)$, $l \neq j$, to $\hat{r}_{i,j}(t)$, and recalculate $\tilde{r}_{i,l}(t)$; for other UEs, since RB_j has already been allocated, their $\tilde{r}_{q,l}(t)$, $q \neq i$ and $l \neq j$, should not be affected by $\hat{r}_{q,j}(t)$. The former is due to the robust rate constraint; the latter is caused by the contiguous constraint.

We again use Fig. 2(a) to illustrate phase 2 operations. Since $\Delta_1(t)$=$\Delta_2(t)$=3-2=1, $\Delta_3(t)$=7-2=5, $\Delta_4(t)$=4-2=2, and$\Delta_5(t)$=5-4=1, we know that $\Delta_3(t)$ is the largest rate gap, and thus RB_3 is the first RB to be allocated, and it is assigned to UE_1 (due to UE_1 has the largest RB rate among three UEs), as shown in Fig. 2(b). Also, even been allocated more RBs, the adopted RB rate of UE_1 will not exceed 7, and thus $\hat{r}_{1,4}(t)$ is adjusted from 8 to 7 (we mark this change by red color). The scheduler further recalculates the corresponding window-constrained RB-rates for UE_2 and UE_3. Note that RB_3 has been allocated to UE_1, and thus it has no impact on the rate updates of UE_2 and UE_3 (we draw these two blocks with black color). For example, for UE_2 and RB_2, $\tilde{r}_{2,2}(t)$= min$\{\hat{r}_{2,1}(t), \hat{r}_{2,2}(t)\}$ = min {3, 3} = 3. All changes are marked with red color, shown in Fig. 2(b).

(3) Phase 3: Selection of next RB and UE candidates

The next RB to be allocated would be either the left or the right neighbor which is exactly next to the "allocated RB block". For example, assume that $\{RB_j, RB_{j+1}, \ldots, RB_l\}$ have already been allocated, and these (l-j+1) RBs form an

i \ j	RB$_1$			RB$_2$			RB$_3$			RB$_4$			RB$_5$		
	$r_{i,j}(t)$	$\hat{r}_{i,j}(t)$	$\tilde{r}_{i,j}(t)$	$r_{i,j}(t)$	$\hat{r}_{i,j}(t)$	$\tilde{r}_{i,j}(t)$	$r_{i,j}(t)$	$\hat{r}_{i,j}(t)$	$\tilde{r}_{i,j}(t)$	$r_{i,j}(t)$	$\hat{r}_{i,j}(t)$	$\tilde{r}_{i,j}(t)$	$r_{i,j}(t)$	$\hat{r}_{i,j}(t)$	$\tilde{r}_{i,j}(t)$
UE$_1$	3	3	3	7	7	3	10	10	7	8	8	4	4	4	4
UE$_2$	3	3	3	5	5	2	2	2	2	10	10	2	5	5	5
UE$_3$	3	3	2	2	2	1	1	1	1	3	3	1	3	3	3

(a) Phase 1: R-Table initialization

i \ j	RB$_1$			RB$_2$			RB$_3$			RB$_4$			RB$_5$		
	$r_{i,j}(t)$	$\hat{r}_{i,j}(t)$	$\tilde{r}_{i,j}(t)$	$r_{i,j}(t)$	$\hat{r}_{i,j}(t)$	$\tilde{r}_{i,j}(t)$	$r_{i,j}(t)$	$\hat{r}_{i,j}(t)$	$\tilde{r}_{i,j}(t)$	$r_{i,j}(t)$	$\hat{r}_{i,j}(t)$	$\tilde{r}_{i,j}(t)$	$r_{i,j}(t)$	$\hat{r}_{i,j}(t)$	$\tilde{r}_{i,j}(t)$
UE$_1$	3	3	3	7	7	3	10	7	7	8	7	4	4	4	4
UE$_2$	3	3	3	5	5	3	2	2		10	10	5	5	5	5
UE$_3$	3	3	2	2	2	2	1	1		3	3	3	3	3	3

(b) Phase 2: the first RB assignment and R-Table updates

i \ j	RB$_1$			RB$_2$			RB$_3$			RB$_4$			RB$_5$		
	$r_{i,j}(t)$	$\hat{r}_{i,j}(t)$	$\tilde{r}_{i,j}(t)$	$r_{i,j}(t)$	$\hat{r}_{i,j}(t)$	$\tilde{r}_{i,j}(t)$	$r_{i,j}(t)$	$\hat{r}_{i,j}(t)$	$\tilde{r}_{i,j}(t)$	$r_{i,j}(t)$	$\hat{r}_{i,j}(t)$	$\tilde{r}_{i,j}(t)$	$r_{i,j}(t)$	$\hat{r}_{i,j}(t)$	$\tilde{r}_{i,j}(t)$
UE$_1$	3	3	3	7	7	3	10	7	7	8	7	4	4	4	4
UE$_2$	3	3	3	5	5	3	2	2		10	10	5	5	5	5
UE$_3$	3	3	2	2	2	2	1	1		3	3	3	3	3	3

(c) Phase 3: selection of next RB and UE candidates

i \ j	RB$_1$			RB$_2$			RB$_3$			RB$_4$			RB$_5$		
	$r_{i,j}(t)$	$\hat{r}_{i,j}(t)$	$\tilde{r}_{i,j}(t)$	$r_{i,j}(t)$	$\hat{r}_{i,j}(t)$	$\tilde{r}_{i,j}(t)$	$r_{i,j}(t)$	$\hat{r}_{i,j}(t)$	$\tilde{r}_{i,j}(t)$	$r_{i,j}(t)$	$\hat{r}_{i,j}(t)$	$\tilde{r}_{i,j}(t)$	$r_{i,j}(t)$	$\hat{r}_{i,j}(t)$	$\tilde{r}_{i,j}(t)$
UE$_1$	3	3	3	7	7	3	10	7	7	8	7	4	4	4	4
UE$_2$	3	3	3	5	5	3	2	2		10	10	5	5	5	5
UE$_3$	3	3	2	2	2	2	1	1		6	6	6	7	7	6

(d) Phase 4: Sum rate estimation

Fig. 2. An illustrative example: operations of the proposed scheduling algorithm

allocated RB block. Let RB$_j$ be assigned to UE$_i$ and RB$_l$ is assigned to UE$_y$. The steps of phase 3 are:

Step 1: Compare $\tilde{r}_{i,j-1}(t)$ and $\tilde{r}_{y,l+1}(t)$. If $\tilde{r}_{i,j-1}(t) \geq \tilde{r}_{y,l+1}(t)$, the next RB is RB$_{j-1}$; otherwise it's RB$_{l+1}$.

Step 2: Assume that the next one is RB$_{j-1}$. If existing some UEs in $\mathcal{N}$ (say UE$_z$) whose $\tilde{r}_{z,j-1}(t) > \tilde{r}_{i,j-1}(t)$, these UEs are candidates to use RB$_{j-1}$. The scheduler stops performing Phase 3 operations and goes to Phase 4.

Step 3: If no UEs in $\mathcal{N}$ (say UE$_z$) whose $\tilde{r}_{z,j-1}(t) > \tilde{r}_{i,j-1}(t)$, while UE$_z$ has the largest $\tilde{r}_{z,j-1}(t)$ among all available RBs, UE$_z$ would be considered as a candidate upon satisfying $(\tilde{r}_{i,j-1}(t) - \tilde{r}_{z,j-1}(t)) - (\tilde{r}_{z,j-1}(t) - \tilde{r}_{z,p}(t)) < 0$, where UE$_z$ has the second largest RB rate in RB$_p$. After verifying all UEs in $\mathcal{N}$, the scheduler stops performing Phase 3 operations to goes to Phase 4.

Step 4: If none UE$_z$ satisfies the condition, the scheduler allocates RB$_{j-1}$ to UE$_i$; it then updates $\mathcal{M} = \mathcal{M} - \{\text{RB}_{j-1}\}$, and $\mathcal{M}' = \mathcal{M}' + \{\text{RB}_{j-1}\}$. If $\mathcal{M} \neq \emptyset$, the scheduler updates R-Table (i.e., Step 5 of Phase 2), and performs Phase 3 operations again.

Again in Fig. 2(c), the assigned RB block only consists of RB$_3$, and thus the scheduler will select either RB$_2$ or RB$_4$ to do scheduling. Since $\tilde{r}_{1,2}(t) < \tilde{r}_{1,4}(t)$, the next RB is RB$_4$. Due to $\tilde{r}_{2,4}(t) > \tilde{r}_{1,4}(t)$, UE$_2$ is the candidate to be allocated RB$_4$.

(4) Phase 4: Sum rate estimation

In this phase, the scheduler calculates all sum RB rates for all possible combinations through forward estimation. Based on the assumption in Phase 3, the detailed steps are:

Step 1: The scheduler sorts all RBs in $\mathcal{M} - \{\text{RB}_{j-1}\}$ in decreasing order of $\tilde{r}_{z,r}(t)$, where RB$_r$ is in $\mathcal{M} - \{\text{RB}_{j-1}\}$.

Step 2: The scheduler forward estimates the sum rates of all combinations. Among all estimated rates, the scheduler allocates RB$_{j-1}$ to the UE which generates a largest rum rate.

Step 3: The scheduler updates $\mathcal{M} = \mathcal{M} - \{\text{RB}_{j-1}\}$, and $\mathcal{M}' = \mathcal{M}' + \{\text{RB}_{j-1}\}$, $\mathcal{N}$ and $\mathcal{N}'$ when needed. If $\mathcal{M} \neq \emptyset$, the scheduler updates R-Table (i.e., Step 5 of Phase 2), and performs Phase 3 operations again.

Since UE$_2$ is the only candidate for RB$_4$ to be allocated to (see Fig. 2(c)), we modify part of the RB rates of UE$_3$, as shown in Fig. 2(d), for well explaining the operations of Phase 4. Now the scheduler performs sum rate estimation for both UE$_2$ and UE$_3$. Considering the case that RB$_4$ is assigned to UE$_2$, and after sorting ($\tilde{r}_{2,5}(t) \geq \tilde{r}_{2,1}(t) \geq \tilde{r}_{2,2}(t)$), the following RBs are RB$_5$, RB$_2$, and RB$_1$, all possible combinations are [(RB$_3$→UE$_1$, RB$_4$→UE$_2$, RB$_5$→UE$_2$, RB$_2$→UE$_1$, RB$_1$→UE$_3$), (18)], [(RB$_3$→UE$_1$,

Table I. Parameter settings of the LTE UL system

Parameter	Setting
System bandwidth	10MHz
Subcarriers per RB	12
Symbols per subcarrier	7
RB bandwidth	180 kHz
Number of RBs	50
Number of active UEs	1 ~ 25
Fading channel	Frequency selective fading
Simulation time	1000 TTIs
Modulation and Coding Scheme	QPSK (1/2, 2/3, 3/4) 16QAM (1/2, 2/3, 3/4) 64QAM (2/3, 3/4)
Window Size	5

$RB_4 \rightarrow UE_2$, $RB_5 \rightarrow UE_2$, $RB_2 \rightarrow UE_3$, $RB_1 \rightarrow UE_3$), (21)], and [($RB_3 \rightarrow UE_1$, $RB_4 \rightarrow UE_2$, $RB_5 \rightarrow UE_3$, $RB_2 \rightarrow UE_1$, $RB_1 \rightarrow UE_1$), (20)], here the first item indicates the allocation, and the second item is the estimated sum rate. On the other hand, RB_4 is assigned to UE_3, and after sorting ($\tilde{r}_{3,5}(t) \geq \tilde{r}_{3,1}(t) \geq \tilde{r}_{3,2}(t)$), the following RBs are still RB_5, RB_2, and RB_1, all possible combinations are [($RB_3 \rightarrow UE_1$, $RB_4 \rightarrow UE_3$, $RB_5 \rightarrow UE_3$, $RB_2 \rightarrow UE_1$, $RB_1 \rightarrow UE_3$), (21)], [($RB_3 \rightarrow UE_1$, $RB_4 \rightarrow UE_3$, $RB_5 \rightarrow UE_3$, $RB_2 \rightarrow UE_2$, $RB_1 \rightarrow UE_2$), (25)], and [($RB_3 \rightarrow UE_1$, $RB_4 \rightarrow UE_3$, $RB_5 \rightarrow UE_2$, $RB_2 \rightarrow UE_1$, $RB_1 \rightarrow UE_1$), (20)]. Based on explored possibilities, the scheduler allocates RB_4 to UE_3, updates all parameters and sets, and goes to Phase 3 again.

IV. Performance Evaluation

In this section, we evaluate and compare the system throughput of proposed heuristic algorithms with Regular-CDS (denotes as CAS) [6]. Besides, two Smart-CDSs are also compared (denotes as TTRA and STRA [7]). The parameter settings are listed in Table I. Herein we use Jain's fairness index [9] as the measurement criterion for data-rate fairness. Each simulation result is the average of 1,000 runs.

We first investigate the throughput performance of four heuristic algorithms, and the result is shown in Fig. 3. The number of deployed UEs varies from 1 to 25, and each TTI consists of 25 RBs. Among four channel-aware scheduling algorithms, the proposed algorithm performs the best. The reason is our approach allocates RBs based on the concept of "rate benefit".

We also investigate the performance of fairness index. In this simulation, we focus on the environment setting of 25 UEs and 100 TTI, and the result is in Fig. 4. For the comparison purpose, we also present the simulation result of without PF support. We observe that as expected, Non-PF-support algorithms perform worse than PF-support algorithms. We further observe that the fairness indices in all methods tend to converge to certain values, respectively, when the number of TTI becomes large, shown in Fig. 5. When the simulation time is longer than 40 TTIs, all algorithms perform similar in terms of the fairness index.

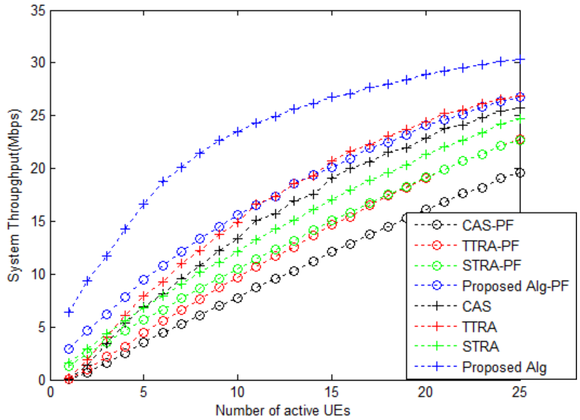

Fig. 3 The performance of system throughput

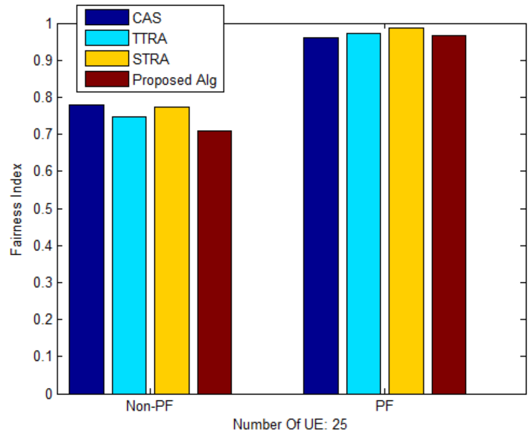

Fig. 4 The performance of fairness index

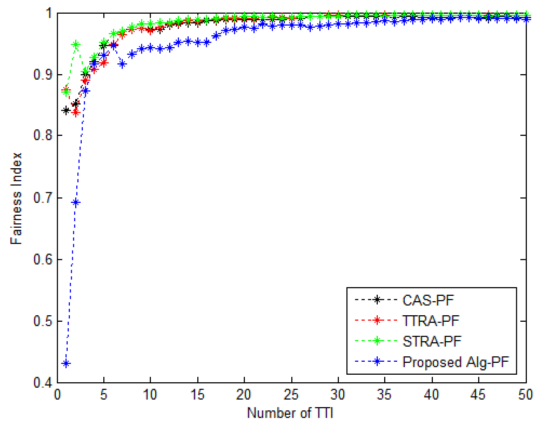

Fig. 5 The change of fairness index

V. Conclusion

In this paper, we first introduce two inherent constraints of SC-FDMA channel access scheme. Herein we name these two constraints "contiguity constraint" and "robust rate constraint". Taking the two constraints into consideration, we formulate the scheduling problem to maximize the sum RB rate. Due to the high computation complexity, we further design a heuristic algorithm.

We not only investigate the system throughput performance, but also performance of fairness index. We find algorithm outperforms the other three approaches with PF and without PF.

Our future work includes: designing a per-UE-based dynamic setting scheme, and improving the estimation accuracy.

REFERENCES

[1] T. Lunttila, J. Lindholm, K. Pajukoski, E. Tiirola, and A. Toskala, "EUTRAN Uplink Performance," International Symposium on Wireless Pervasive Computing (ISWPC) 2007, February 2007.

[2] Moray Rumney, "3GPP LTE: Introducing Single-Carrier FDMA," Agilent Measurement Journal, 2008.

[3] Stefania Sesia, Issam Toufik, Matthew Baker, "LTE-the UMTS Long Term Evolution From Theory to Practice."

[4] J. Lim, H. Myung, K. Oh, and D. Goodman, "Proportional Fair Scheduling of Uplink Single-Carrier FDMA Systems," Proceedings of IEEE Personal, Indoor and Mobile Radio Communications (PIMRC) 2006, pp.1-5.

[5] Suk-Bok Lee, Ioannis Pefkianakis, Adam Meyerson, Shugong Xu, and Songwu Lu, "Proportional Fair Frequency-Domain Packet Scheduling for 3GPP LTE Uplink," Proceedings of IEEE International Conference on Computer Communications (INFOCOM) 2009, pp. 2611-2615.

[6] L. R. deTemino, G. Berardinelli, S. Frattasi, and S. Mogensen, "Channel-aware Scheduling Algorithms for SC-FDMA in LTE Uplink," Proceedings of IEEE Personal, Indoor and Mobile Radio Communications (PIMRC), 2008, pp. 1-5.

[7] Ching-Hsu Chang, Hsi-Lu Chao, and Chia-Lung Liu, "Resource Allocation with Sum Throughput Improvement for LTE Uplink Transmission," Proceedings of IEEE Vehicular Technology Conference (VTC) 2011 Fall, pp.1-5.

[8] Erik Dahlman, Stefan Parkvall, Johan Skold, and Per Beming, "3G Evolution: HSPA and LTE for Mobile Broadband."

[9] R. Jain, D. M. Chiu, and W. Hawe, "A Quantitative Measure of Fairness and Discrimination for Resource Allocation in Shared Systems," Technical Report TR-301, DEC Research Report, 1984.